ASYMMETRY IN A CONFINED RECTANGULAR JET IN CROSSFLOW

David M. Cusano[†] and Michael W. Plesniak
School of Mechanical Engineering
Maurice J. Zucrow Laboratories
Purdue University
West Lafayette, IN 47907-1288, USA

ABSTRACT

The development of a rectangular jet of fixed aspect ratio issuing into a rectangular duct was studied. This is a specialized case of jets in crossflow (JICF) of interest in manufacturing processes. The jet is confined in the spanwise and cross-stream directions and the mass flux ratio between the two streams is high. The particular emphasis of this paper is on the asymmetric states that develop as the flow evolves. A Mie-scattering-based technique was used to make scalar concentration field measurements. A full factorial test matrix was employed in order to investigate the relative effects of three parameters: jet to crossflow velocity ratio, injection angle, and downstream distance. An increasingly pronounced asymmetry in the scalar concentration field was found in the 30° and 48° injection angle cases, and worsened for injection angles greater than 48°. These results, combined with laser Doppler velocimetry measurements, showed that the primary flow structure, the counter-rotating vortex (CRV) pair was asymmetric. No asymmetries were found in the inlet or boundary conditions of the experiment. Furthermore, perturbations, such as introducing small skew angles were unsuccessful in altering the basic character of the asymmetry. This leads to the conclusion that this flow geometry preferentially produces asymmetric flow fields. The high degree of confinement is believed to make the flow more prone to the asymmetric states than unconfined JICF.

INTRODUCTION

Jets discharging into crossflows are common in many engineering applications. Some examples include: effluents issuing from smoke stacks and chimneys, waste water discharge into moving bodies of water, V/STOL aircraft in transition flight, dilution zones in gas turbine combustors, cooling of turbine blades, gaseous state fuel injection, and numerous manufacturing processes. Because of the wide range of applications, the literature is extensive (see reviews by Sherif & Pletcher, 1990; Margason, 1993; Holdeman, 1993). Many important features of this flow field, such as jet trajectory, spreading rates and momentum ratio effects have been investigated and characterized. Despite the extensive research spanning over five decades, basic understanding of the flow physics is still incomplete.

The important parameters influencing the behavior of unconfined jets in crossflow are momentum ratio, injection angle, and skew angle. Rectangular jets are also influenced by jet aspect ratio (AR), particularly for AR > 1.0. All of these parameters affect the development of the main counter-rotating vortex (CRV) pair, which is the structure primarily responsible for jet trajectory, entrainment, and large-scale transport, or mixing. Confinement of JICF has received little attention. Only mild confinement has been studied with mass flux ratio, MR ≈ 0.1. The present study has MR between 0.17 and 0.53.

Over the wide range of parameters explored, many authors have reported two distinct regimes of jet behavior: the wall jet and fully lifted jet regimes (e.g. Sherif and Pletcher, 1990). Some authors also report a transitional regime between these two (e.g. Sherif and Pletcher, 1991; Lim, et al., 1994. The wall jet is usually associated with a lack of strong CRV, weak wake development and little mixing. The fully lifted jet penetrates the boundary layer of the wall and contains strong wake vortices, as well as the CRV pair. There is a growing body of evidence indicating that the flow field created by a jet in crossflow is not

[†] currently at AFAB Technologies, Inc., 11420 Fortune Circle, Suite 3, West Palm Beach, FL 33414

inherently symmetric (even in the mean sense). Many researchers have shown that the CRV structures vary in size, location and strength (e.g. Rathgeber & Becker, 1983). Recently reported work by Kuzo (1995) and Smith & Mungal (1998) revealed that the basic flow associated with a single unconfined round jet in crossflow may have associated with it very complex asymmetric states. These studies indicate that symmetric geometries can produce flows that are symmetric (in the mean) for certain flow conditions and streamwise locations, but are asymmetric for other conditions and streamwise locations.

The present configuration consisting of a confined rectangular jet in crossflow is unique in that the planar jet spans almost 80% of the crossflow duct and that the jet is confined in the cross-stream direction as it issues into a relatively narrow duct. The objective of this study was to investigate the development and evolution of coherent structures, created by this geometry, over a large parameter space. Velocity fields information was obtained for conditions of transitional behavior. The particular emphasis of this paper is on the asymmetric flow field.

EXPERIMENTAL APPARATUS AND TECHNIQUES

The clear Plexiglas flow facility allows complete access for optical diagnostics. It consists of a main duct partially intersected along one sidewall by a secondary duct from which the jet issues. The main duct measures 7.62 cm high, 5.72 cm wide and 3.96 m long, while the secondary duct is 6.05 cm high, 2.54 cm wide and 0.91 m long. Both streams are supplied by a compressed air source through electrically-actuated, computer-controlled valves, and monitored with orifice plates/pressure transducers (see Eaton, et al. 1996). The velocity in the ducts ranges from 50 to 80 m/s, with Reynolds numbers based on hydraulic diameter on the order of 2×10^5.

Each duct had a inlet plenum containing flow conditioners and a 2-D nozzle. At the end of the test section, an exit diffuser is used to transition back to round piping. Both ducts were designed to have fully developed velocity profiles upstream of their intersection to achieve well-defined inflow boundary conditions. Complete details concerning the design and performance of the flow facility are in Cusano (1999). The length scale used for nondimensionalization is the hydraulic diameter of the secondary duct (jet).

Measurement Techniques

A full-field, planar Mie-scattering-based optical diagnostic technique developed by Eaton et al. (1996) in our laboratory was used in the present study. Al_2O_3 tracer particles were introduced into the secondary duct, well upstream of the inlet plenum, to mark the jet fluid. The jet fluid concentration is inferred from the measured intensity distribution resulting from Mie scattering by the tracer particles. Results of Samimy and Lele (1991) indicate that for these flow conditions ($\tau = 0.46$, τ = particle response time divided by the fluid response time, and Sc=0.8, Sc = Schmidt number) the size of particles used (0.3 - 1.0 microns) will faithfully track the motion of the flow, with no influence from diffusion or inertia. Particle settling due to gravity is negligible because of the initial uniformity of flow seeding and the extremely short transit time (typically 3 - 25 ms) to reach the measurement locations.

The imaging system consists of: two digital cameras, a computer with two frame grabber boards, a pulsed ruby laser, and a laser fluorescent dye cell. The pulsed ruby laser beam is expanded into a sheet and used to illuminate the plane of interrogation. The two cameras are operated simultaneously: a 10-bit, 1.6 mega-pixel digital camera captures the mixing images while a analog CCD camera records the laser energy profile by imaging the dye cell containing a dilute solution of laser fluorescent dye. After image acquisition, image-processing software is used to correct the mixing image for variations in the laser sheet energy profile, the solid and scattering angle variations across the image and electronic noise. Figure 1 shows a plan-view schematic of the apparatus and an example processed scalar concentration map. The image is shown from the perspective of the mixing image camera. Thus, the main flow is coming out of the page, while the marked jet fluid enters from the left side of the image. All subsequent figures are plotted in this orientation.

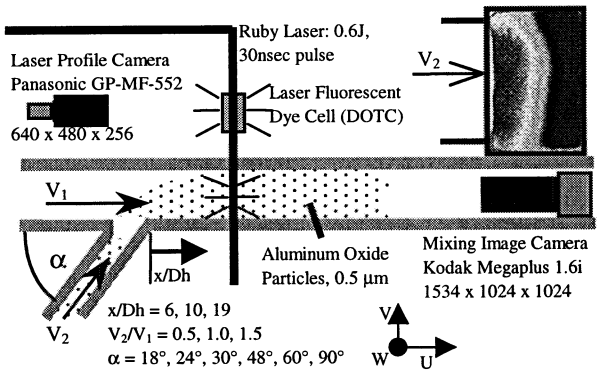

Figure 1. Mie Scattering Based Imaging System Schematic

A Dantec two-component fiber optic LDV system was used to acquire velocity data. This system included: a fiber optic LDV probe, a three-axis computer-controlled motorized traverse and a FVA type signal processor. To obtain three dimensional data, the probe was oriented in two orthogonal planes allowing all three velocity components to be acquired, two at a time. The U-V plane (defined in Figure 1) data were taken with the beams propagating through the sidewall. The U-W plane data were taken by reflecting the beams off of a mirror oriented at 45° from horizontal and mounted directly under the test section. Using this configuration facilitated alignment of the two measurement planes.

Experimental Uncertainty

Within an individual image, the total uncertainty for the Planar Mixing Diagnostic System is ±2.1% (affects the shape of the particle cloud in an image). Details of the uncertainty analysis are provided in Cusano, (1999). When comparing images from different realizations, the error increases due to particle seeding fluctuations. The seed particle concentration fluctuations were measured by Eaton, et al. (1996) to be ±5%. This increases the uncertainty of the measurements to ±7% (affects the accuracy of the mean grey level from image to image).

RESULTS AND DISCUSSION

A full factorial test matrix was employed in order to investigate the relative effects of three parameters: jet to crossflow velocity ratio, injection angle, and downstream distance. Three velocity ratios (Vr = 0.5, 1.0, 1.5), three downstream distances (x/D_h = 6, 10, 19) and 6 angles (18°, 24°, 30°, 48°, 60°, 90°) were investigated in all possible combinations for a total of 54 experiments.

The results of the full factorial experiments (Cusano, 1999; Cusano & Plesniak, 1996) showed the onset of a pronounced asymmetry in the mean scalar concentration field in the 30°and 48° injection angle cases. These results further prompted additional investigation of the 30° and 48° cases using LDV.

Scalar Concentration Field

To quantify mixing, sets of 15 to 20 individual images were acquired and averaged to form a composite image, or scalar concentration map (SCM). The composite image was normalized by the average intensity, which represents a perfectly mixed value, assuming ideal mixing. This normalization enables results to be compared directly among the various cases. Within each grouping of images there are three columns corresponding to (from left to right) Vr = 0.5, 1.0 and 1.5 with the three rows corresponding to (from top to bottom) x/D_h = 6, 10 and 19. While composite images provide a measure of time-averaged scalar field behavior, the time-varying or unsteady information is lost. Previous studies have shown that the CRVs often fluctuate in size and location (usually in an asymmetric fashion). To quantify this important quality of the flow field, concentration fluctuation maps (CFMs) were calculated for the data set following the procedure of Rathgeber and Becker (1983). Concentration fluctuation is defined as:

$$C' = \frac{\hat{\gamma}}{C_{mean}} \qquad (1)$$

where $\hat{\gamma}$ = RMS value of C about C_{mean} where C_{mean} is the average concentration.

Results for α = 30°. The mean and fluctuating concentration distributions for the 30° injection angle are shown in Figure 2. For low Vr and x/D_h , the 30° case behaves like the lower angle (18° and 24°) cases (Cusano, 1999). The SCM exhibit increased cross-stream penetration with downstream distance, as indicated by the displacement of the concentration contours (dark regions denote absence of tracer particles, or jet fluid). The corresponding CFM (Figure 2b) depict patterns consistent with the existence of CRV pairs (middle and left columns). That is, the CRV pair causes high concentration fluctuations in its vicinity, i.e. on either end of the kidney-shaped cross section of the jet, and regions of lower fluctuations near the middle of the kidney. These signatures are very clear in the Vr = 1.0 and 1.5 cases. For higher Vr and x/D_h the SCM begins to exhibit a very different character shown in the lower right of Figure 2a. At x/D_h = 10, the particle cloud marking the jet fluid (near-white regions) begins to be skewed towards the lower wall and by x/D_h = 19 the particle cloud appears to anchor itself on the injection wall-floor junction (lower left corner of image).

Results for α = 48°. Like the lower angle cases, the Vr = 0.5 SCM (Figure 3a) show little evidence of large-scale transport across the duct. At this low velocity ratio the CRV pair is expected to be weak, resulting in little mixing. The CFM (Figure 3b) show organized regions of high fluctuations at all downstream locations, the signature of the CRV pair. The existence of these organized regions at x/D_h = 19 (Figure 3b lower-left) indicates that although weak, the CRV pair persists far downstream. The regions of high scalar concentration near the injection wall shown in the SCM and the coherent structure shown in the CFM, are indications that the jet starts out lifted from the injection wall then "reattaches" at some point downstream. This condition allows the CRV pair to become more developed than in the lower angle (wall jet regime) cases, causing the scalar field to become better mixed as downstream distance increases. Flow visualization confirmed a change in jet wake structure, affirming that a new regime has been entered (Cusano, 1999).

In the Vr =1.5 cases, the jet appears to be elevated or "lifted" from the wall, as particle-rich regions of the SCM depict the classical kidney-shaped cross section for the first time (top-right Figure 3a). The majority of entrainment in JICF occurs along the jet spanwise centerline on the injection side of the jet. The CRV pair acts to "pump crossflow fluid into the center of the jet. Entrainment results in a locally well-mixed condition shown by regions of grey in the SCM. The CRV pair, for this case, is much stronger than in previously discussed cases resulting in the large grey regions at x/D_h = 6 (Figure 4, top-right). By the last measurement location, x/D_h = 19, the flow is very well mixed across the entire duct, but asymmetric from top to bottom.

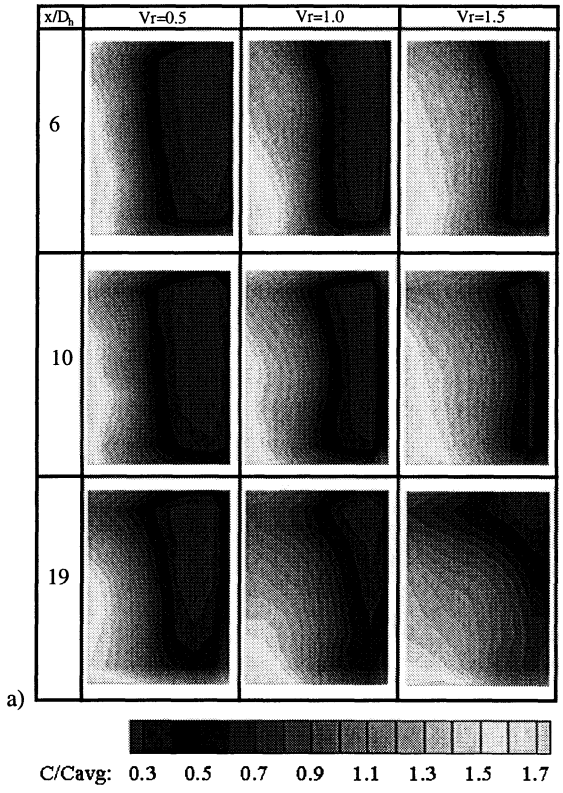

Figure 2. a) Mean Concentration maps b) Concentration fluctuation maps for $\alpha = 30°$, Vr=0.5, 1.0 and 1.5, x/Dh=6,10 and 19

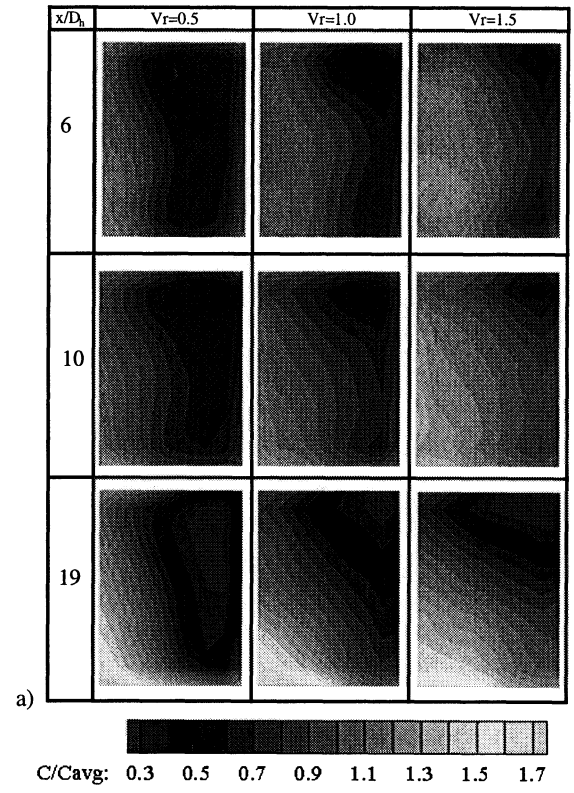

Figure 3. a) Mean Concentration maps b) Concentration fluctuation maps for $\alpha = 48°$, Vr=0.5, 1.0 and 1.5, x/Dh=6,10 and 19

Velocity Data

Results for α = 30°. At station x/D_h=6, Vr=1.0 (Figure 4a, left-most image), the high-speed core of the main flow has been displaced from the injection wall. Secondary velocity vectors in the core have nearly zero magnitude, indicating that the jet is aligned with the crossflow. Organized secondary flows both upwards and downwards towards the injection wall begin to develop. Further downstream, measurement planes x/D_h=10 and 19 show the results of the jet-crossflow interaction. The low momentum fluid near the injection wall mixes with the crossflow fluid. This occurs near the centerline of the duct where jet entrainment is highest, resulting in the cusp shaped velocity core. The core is asymmetric from top to bottom in the duct, with the bulk of the flow located towards the bottom of the image. The secondary velocity field is much more symmetric than the streamwise velocity for this case.

For Vr = 1.5 (Figure 4b), the jet velocity is 50% higher than the crossflow velocity so the jet appears as the high velocity region near the injection wall. At x/D_h=6 the difference between the Vr = 1.0 and Vr = 1.5 cases is enormous, as the action of the CRV pair dominates the flow field. The center of the flow field shows no indication of the high velocity jet fluid. Entrainment has already mixed the streamwise momentum of the two unequal velocity streams. Two cores of high velocity jet fluid (indicated by the white regions),which generally correspond with the centers of the CRV pair, are apparent. The maximum velocity in the two cores is not equal, with the velocity closest to the top of the duct greater, opposite to the trend found in the Vr=1.0 case. The secondary velocity field shows two very well defined, organized CRVs. These structures are also asymmetric. The lower vortex is located close to the middle of the duct and is much larger than the upper vortex.

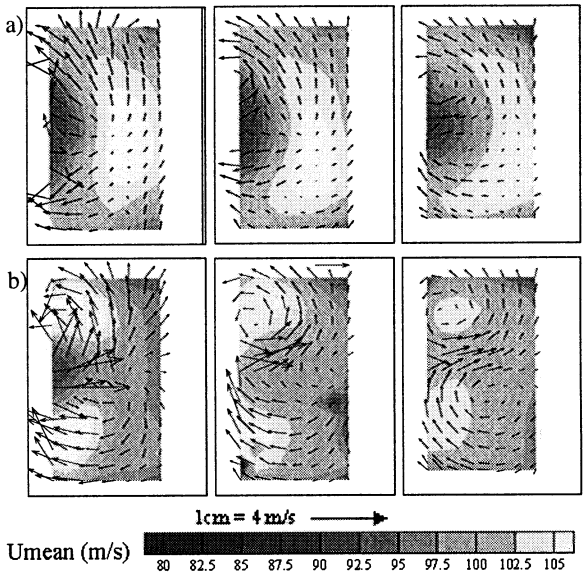

Figure 4. Mean velocity field results for a) Vr=1.0 and b)Vr=1.5 for α = 30°, x/Dh=6,10 and 19

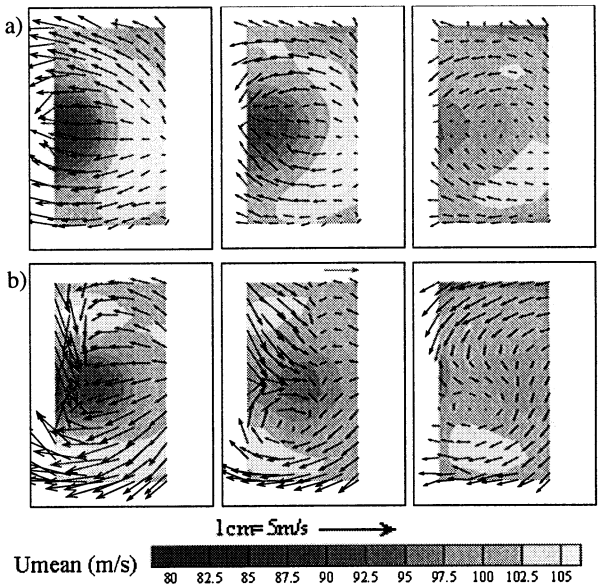

Figure 5. Mean velocity field results for a) Vr=1.0 and b)Vr=1.5 for α = 48°, x/Dh=6,10 and 19

Results for α = 48°. The effect of increasing injection angle on the mean velocity field is apparent immediately at x/D_h = 6 for Vr=1.0 (Figure 5a). There is a well-defined, low momentum region corresponding to the jet (black area near the injection wall). The observed trends are the same as for the 30° case, except that the entrainment appears to be much stronger, as indicated by the size and growth of the low momentum region (dark region). By x/D_h = 19, the streamwise mean velocity is nearly mixed out (approaching fully developed duct flow distribution). This contrasts the 30°, x/D_h = 19, Vr=1.0 case which had only reached a level of mixedness comparable to the 48° x/D_h = 10 case (compare Figures 4a and 5a). Increasing the injection angle from 30° to 48° results in halving the streamwise distance required to achieve the same amount of large scale mixing. The Vr=1.5 case (Figure 5b) shows a high degree of entrainment immediately at x/D_h = 6. The jet core is already "split" with an extremely strong low momentum (negative U_{mean} velocities not discernable on plot). The twin jet cores are still evident but much less distinguishable region in the center. This low momentum region is in the "wake" of the jet as reversed flows were measured here than in the 30° case due to the higher level of entrainment. The twin cores are asymmetric as before but the bottom core is the stronger of the two. Secondary velocity field also becomes highly asymmetric for as in the Vr=1.5, 30° case. The upper vortex is nearly non-existent in the mean with the lower vortex dominating the entire flow field.

Asymmetry Investigation

Extensive benchmarking of the apparatus and inlet flow conditions verified that they were symmetric in all measurable respects. The source of the asymmetry was not obvious, so a search for clues to its origins was undertaken. Many tests (e.g. flipping the entire test section, offsetting the jet spanwise, etc.) were tried to eliminate or reverse the asymmetry with no success. See Cusano (1999) for a complete description of the asymmetry investigation.

The literature suggests that one way of producing an asymmetric vortex pair with JICF is to skew the jet. The skewed jets produced pairs of highly asymmetric vortices of unequal size (e.g. Liscinsky et al., 1994; Johnston & Khan, 1997; Compton & Stadnicki, 1998; Wu, et al., 1991). A study was performed in which the duct was skewed a known finite amount (skew angles of -2° and +3°) to test if the presence of an unintentional, almost imperceptible skew of the secondary duct was responsible for the asymmetry. The effect of skew angle, while changing the details of the scalar concentration, did not change the basic character of the asymmetry. For example, the asymmetric distribution could not be flipped top to bottom. These results, in light of the work of Smith and Mungal (1998) and Kuzo (1995), support their conclusion that the asymmetric solution is a natural state of the flow.

CONCLUSIONS

The velocity and scalar concentration fields in a confined rectangular jet in crossflow were measured. Asymmetries in the distribution of jet fluid marked by tracer particles were found over a large portion of the parametric space investigated. As the jet transitioned from a "wall jet" to a "lifted jet" behavior, (for conditions in 30° and 48° cases) the flow field became increasingly asymmetric. The asymmetric behavior became more pronounced as jet penetration increased with increasing velocity ratio, and injection angle. LDV measurements, showed that the primary flow structure, the counter-rotating vortex pair was asymmetric in strength, size, and position. No asymmetries were measurable in the inlet or boundary conditions of the experiment. Furthermore, small skew angles and other perturbations, while having an effect, did not alter the basic character of the asymmetry. This leads to the conclusion that this flow configuration preferentially produces asymmetric flow fields. The high degree of confinement in this flow makes the jet more susceptible to asymmetries than its unconfined counterpart.

ACKNOWLEDGMENTS

The authors are grateful for the support provided by the Procter & Gamble Co.

REFERENCES

Compton, D. A., Stadnicki, J.P. (1998) "Near Field Flow Visualization of Vortex Generator Jets," ASME paper FEDSM98-4894.

Cusano, D. M. (1999), Studies of a Confined Rectangular Jet in Crossflow, Ph.D. thesis, Purdue University.

Cusano, D. M., Plesniak, M. W. "Mixing of a Rectangular Jet in a Confined Rectangular Crossflow," *Bulletin of the American Physical Society* V. 41, No. 9 (1996), p 1686.

Eaton, A. R., Frey, S. F., Cusano, D. M., Plesniak, M. W., Sojka, P. E. (1996), "Development of a Full-Field Planar Mie Scattering Technique for Evaluating Swirling Mixers," *Experiments in Fluids*, **21**, pp. 325-330.

Holdeman, J. D. (1993), "Mixing of Multiple Jets with a Confined Subsonic Crossflow," *Prog. Energy Combustion Sci.*, **19**, pp. 31-70.

Johnston, J.P., Kahn, Z. (1997) "The Origins of a Dominant Vortex from a Pitched and Skewed Jet," JSME International Conference on Fluids Engineering, July 1997, Tokyo.

Kuzo, D.M. (1995) An Experimental Study of the Turbulent Transverse Jet, Ph.D. thesis, California Institute of Technology.

Lim, T. T., Kelso, R. M., Perry, A. E. (1992) "A Study of a Round Jet in Cross-Flow at Different Velocity Ratios," 11th Australasian Fluid Mechanics Conference, University of Tamania, Hobart, Australia, December 14-18.

Liscinsky, D. S., True, B., Holdeman, J. D. (1996), "Crossflow Mixing of Noncircular Jets," *Journal of Propulsion and Power*, **12**-2, pp. 225-230.

Margason, R. J.(1993), "Fifty Years of Jet in Cross-Flow Research", Presented at Computational and Experimental Assessment of Jets in Cross-Flow, AGARD-CP 534, pp. 1-41.

Rathgeber, D. E., Becker, H. A. (1983), "Mixing Between a Round Jet and a Transverse Turbulent Pipe Flow," *The Canadian Journal of Chemical Engineering*, **61**, pp. 148-157.

Samimy, M., Lele, S. K. (1991), "Motion of Particles with Inertia in a Compressible Free Shear Flow," *Physics of Fluids A*, **3**, pp. 1915-1923.

Sherif, S. A., Pletcher, R. H. (1990),"The Physical and Thermal Characteristics of the Subsonic Jet in a Cross Stream--A Review," *Mixed Convection and Environmental Flows*, **152**, pp. 83-94.

Sherif, S. A., Pletcher, R. H. (1991), "Jet-Wake Thermal Characteristics of Heated Turbulent Jets in Crossflow," *Journal of Thermophysics*, **5**-2, pp. 181-191.

Smith, S.H., Mungal, M.G. (1998) "Mixing, Structure and Scaling of the Jet in Crossflow," *J. Fluid Mech.* **357**, pp. 83-122.

Wu, J. M., Vakili, A. D., Yu, F. M. (1988), "Investigation of the Interacting Flow of Nonsymmetric Jets in Crossflow," *AIAA Journal*, **26**-8, pp. 940-947.